

Shear flow and Kelvin-Helmholtz instability in superfluids

R. Blaauwgeers^{1,2}, V. B. Eltsov^{1,3}, G. Eska^{1,4}, A. P. Finne¹, R. P. Haley^{1,5}, M. Krusius¹, J. J. Ruohio¹,
L. Skrbek^{1,6}, and G. E. Volovik^{1,7}

¹*Low Temperature Laboratory, Helsinki University of Technology, P.O.Box 2200, FIN-02015 HUT, Finland*

²*Kamerlingh Onnes Laboratory, Leiden University, P.O.Box 9504, 2300 RA Leiden, The Netherlands*

³*Kapitza Institute for Physical Problems, Kosygina 2, 117334 Moscow, Russia*

⁴*Physikalisches Institut, Universität Bayreuth, D-95440 Bayreuth, Germany*

⁵*Department of Physics, Lancaster University, Lancaster, LA1 4YB, UK*

⁶*Joint Low Temperature Laboratory, Institute of Physics ASCR and Charles University, V Holešovičkách 2,
180 00 Prague, Czech Republic*

⁷*Landau Institute for Theoretical Physics, Kosygina 2, 117334 Moscow, Russia*
(October 29, 2018)

The first realization of instabilities in the shear flow between two superfluids is examined. The interface separating the A and B phases of superfluid ^3He is magnetically stabilized. With uniform rotation we create a state with discontinuous tangential velocities at the interface, supported by the difference in quantized vorticity in the two phases. This state remains stable and nondissipative to high relative velocities, but finally undergoes an instability when an interfacial mode is excited and some vortices cross the phase boundary. The measured properties of the instability are consistent with a modified Kelvin-Helmholtz theory.

Instabilities in the shear flow between two layers of fluids [1] belong to a class of interfacial hydrodynamics which is attributed to many natural phenomena. Examples are wave generation by wind blowing over water [2], the flapping of a sail or flag in the wind [3,4], and even flow in granular beds [5]. In the hydrodynamics of inviscid and incompressible fluids the transition from calm to wavy interfaces is known as the Kelvin-Helmholtz (KH) instability [6,2]. Since Lord Kelvin's treatise in 1871, difficulties have plagued its description in ordinary fluids, which are viscous and dissipative. They also display a shear-flow instability, but its correspondence with that in the ideal limit is not straightforward. The tangential velocity discontinuity in the shear-flow instability is created by a vortex sheet. In a viscous fluid a planar vortex sheet is not a stable equilibrium state and not a solution of the hydrodynamic equations [7].

Superfluids provide a close variation of the ideal inviscid limit considered by Lord Kelvin and thus an environment where the KH theory can be tested. The initial state is a non-dissipative vortex sheet – the interface between two superfluids brought into a state of relative shear flow. So far the only experimentally accessible case where this can be studied in stationary conditions, is the interface between ^3He -A and ^3He -B [8], where the order parameter changes symmetry and magnitude, but is continuous on the scale of the superfluid coherence length $\xi \sim 10\text{ nm}$. We discuss an experiment, where the two phases slide with respect to each other in a rotating cryostat: ^3He -A performs solid-body-like rotation while ^3He -B is in the vortex-free state and thus stationary in the laboratory frame. While increasing the rotation velocity Ω , we record the events when the AB phase boundary be-

comes unstable – when some circulation from the A-phase crosses the AB interface and vortex lines are introduced into the initially vortex-free B phase. On increasing the rotation further, the instability occurs repeatedly. Such a succession of instability events can be understood as a spin-up of ^3He -B by rotating ^3He -A.

Our experimental setup is shown in Fig. 1. The AB boundary is forced against a magnetic barrier in a smooth-walled quartz container, by cooling the sample below T_{AB} at constant pressure in a rotating refrigerator. The number of vortices in both phases is independently determined from the simultaneously measured nuclear magnetic resonance (NMR) spectra [9,10]. By tuning the barrier field or the temperature, the state of the sample can be changed from all A phase to all B phase or to a two-phase configuration. The evolution of the quantized vorticity as a function of Ω is then observed to be radically different when the AB interface is present.

The quasi-isotropic ^3He -B supports singly quantized vortices with a core size comparable to ξ [9]. In the anisotropic ^3He -A we form vortex lines [10] with continuous skyrmion topology: Inside its central part the order-parameter amplitude remains constant but the axis of the orbital anisotropy covers a solid angle of 4π . Such a “soft-core” structure carries continuous vorticity with two circulation quanta and is three orders of magnitude larger than the core of the B-phase vortex. Thus converting an A-phase vortex into a B-phase vortex requires large concentration of the flow energy.

The large difference in core radii is the origin for the much lower rotation at which vortices start forming in A phase at the outer sample circumference, compared to B phase [9]. If the sample consists of only B phase then the

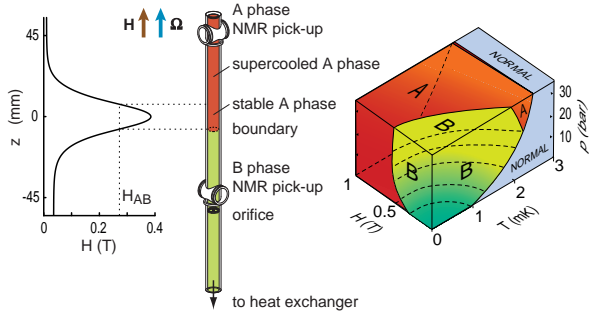


FIG. 1. Stabilization of the first-order $^3\text{He-A} - ^3\text{He-B}$ phase boundary. At pressures $p \geq 21$ bar, A-phase extends to lower temperatures in external magnetic field (see phase diagram on the right). The sample (length 11 cm, radius $R = 0.3$ cm) is first cooled to A phase. On further cooling, the A \rightarrow B transition happens in the coldest place at the bottom. The AB boundary then starts to move up and rises to a height z where the barrier field $H(z)$ equals the value of the thermodynamic A \rightarrow B transition $H_{AB}(T, p)$. The A phase in the top section remains in a metastable supercooled state [11]. Ultimately, the boundary disappears when $H_{AB}(T, p) > [H(z)]_{\max}$. For $p = 29.0$ bar and $H(z)$ as shown in the figure with a current of 4 A in the barrier solenoid, the stable AB boundary exists below 2.07 mK down to 1.33 mK. The NMR spectrometers operate in homogeneous static magnetic fields of 10 mT and 35 mT, chosen for best measuring sensitivity of the single-vortex signal.

critical velocity for forming the first vortex line in the setup of Fig. 1 is $v_{cB} > 7$ mm/s [12], while the critical velocity v_{cA} is a factor of 20 smaller [13], independently of the presence of the AB boundary.

Vortex lines are thus easily created at low rotation in the A-phase section of the sample, while no vortices are detected in the B phase section. This is the ideal non-dissipative initial state where the two superfluid phases slide along each other without friction. When Ω is increased further, sudden bursts of vortex lines are observed in the B-phase section, as shown in Fig. 2. The onset Ω_c depends on temperature and on the current in the barrier magnet. Overall, the measured characteristics of the bursts fit a shear flow instability, which provides a mechanism for the circulation to cross the AB interface.

$^3\text{He-A}$ and $^3\text{He-B}$ are states of the same order-parameter manifold. One of the conditions on their phase boundary is that the phase of the order parameter has to be continuous [14]: If the circulation is not continuing across the interface (Fig. 3A) then the existing A-phase vortex lines have to bend and form a vortex layer on the AB interface. This is the only hydrodynamically stable state, with vortex-free flow seen by the B-phase spectrometer and a large cluster of vortex lines detected by the A-phase spectrometer. The build up of a sheet-like vortex layer means that the A-phase circulation cannot easily penetrate into the vortex-free B-phase and the AB interface remains stable up to the measured critical ve-

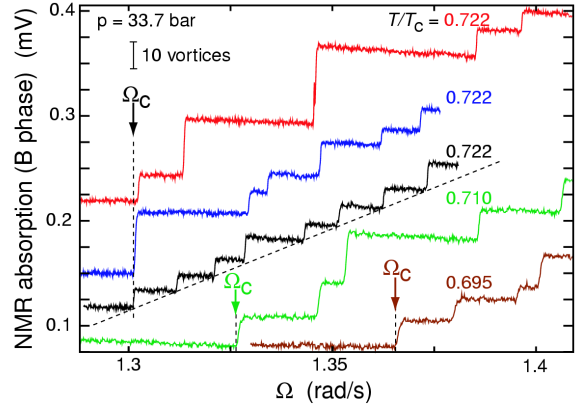


FIG. 2. Instability events during slowly increasing rotation ($d\Omega/dt = 2.5 \cdot 10^{-4}$ rad/s²). NMR absorption signals as a function of Ω are recorded (shifted arbitrarily on the vertical scale). The vertical jumps mark events in which δN new vortex lines enter the B phase section of the sample. The height of each jump is proportional to δN , a small stochastic number. When averaged over a large interval of Ω , the number of B-phase vortex lines grows linearly with Ω . This is demonstrated also by the dashed line: the instability occurs independently of Ω at constant critical drive, *ie.* $u_c = |v_{sB} - v_n|_{r=R} = \Omega_c R = \text{const}$. The three top most signal traces were recorded at the same temperature, *ie.* measurements at fixed T yield the same Ω_c (if small variations in v_{cA} are accounted for [13]). The two bottom traces at different T illustrate that Ω_c depends on temperature. Here $T_{AB}(H = 0) = 0.785 T_c$.

locity $u_c = \Omega_c R \sim 2 - 4$ mm/s $< v_{cB}$.

At $\Omega > \Omega_c$, some vortex lines have broken through the AB phase boundary. Thus there exists also a stable configuration in which vortices from the A phase continue into the B phase, where they form a cluster in the center (Fig. 3B). The likely topology of the intersection is illustrated in Fig. 3C. Thus, although the AB interface is not directly monitored by the two NMR spectrometers, the hydrodynamically stable states below and above Ω_c can only be the configurations in Fig. 3. By comparing B-phase vortex-line creation in the presence and absence of the AB interface, we conclude that the events in Fig. 2 originate from the AB phase boundary.

In the classical KH instability the interface between fluids with densities ρ_1 and ρ_2 becomes destabilized by inertial effects, which are normally balanced by gravity g and surface tension σ . The relative velocity $|v_2 - v_1|$ acts as a drive. When it reaches a critical value [2] given by

$$\frac{\rho_1 \rho_2}{\rho_1 + \rho_2} (v_2 - v_1)^2 = 2\sqrt{\sigma F}, \quad (1)$$

where $F = g(\rho_1 - \rho_2)$ is the gravitational restoring force, waves with wave vector $k = \sqrt{F/\sigma}$ are created on the interface.

This approach can be generalized for superfluids in terms of two-fluid hydrodynamics [15]. For superfluid

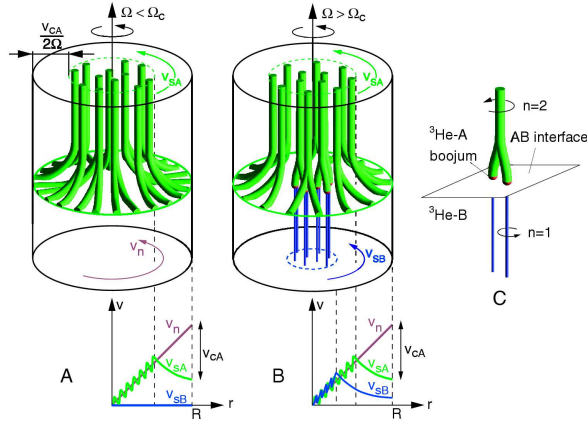


FIG. 3. The two configurations of vortex lines with the AB boundary in rotation. **(A)** $\Omega < \Omega_c$: Vortex lines are formed in $^3\text{He-A}$ while $^3\text{He-B}$ remains vortex-free. Near the AB boundary the A-phase vortices bend parallel to the interface and form a vortex sheet between the sliding superfluids. The radial distributions of the normal and superfluid velocities far from the AB interface are depicted below, with $v_{nA} = v_{nB} = \Omega r$, while $v_{sB} = 0$. **(B)** $\Omega \geq \Omega_c$: Vortices are observed to appear in the B phase in events of a few lines at a time. They form a central cluster in the B-phase section. **(C)** A hydrodynamically stable state with respect to externally imposed perturbations in Ω , T , or H exists at the AB interface for $\Omega \geq \Omega_c$. A topologically stable configuration for the vortex-line intersection with the AB interface is suggested in Ref. [14]: The doubly quantized A-phase vortex terminates at the AB interface in two point singularities, known as boojums. These, in turn, are the end points of two singly quantized B-phase vortices.

^3He under our experimental conditions it is safe to assume that the normal fractions are always in solid-body rotation. Instead of gravity, the restoring force is now produced by the magnetic barrier $H(z)$, owing to the difference in the susceptibilities χ_A and $\chi_B(T, H)$: $F = (1/2)(\chi_A - \chi_B(T, H))\nabla(H^2)$ at $H_{AB}(T)$. The restoring force can thus be calculated as a function of temperature and current in the barrier solenoid. The motion of the AB interface with respect to the normal component is subject to a finite damping [16]. Since the initial state is non-dissipative, damping does not explicitly appear in the stability condition, but modifies the build-up rate of the interface perturbations when the instability develops. The onset of the instability can be derived from the dynamics of small amplitude perturbations, as Eq. (1) is generally derived in textbooks [1], or from the thermodynamics when perturbations of the interface lead to a negative free energy in the rotating frame. The mode for which the interface first becomes unstable has the same wave vector $k = \sqrt{F/\sigma}$ as before at a drive given by

$$\frac{1}{2}\rho_{sA} (v_{sA} - v_n)^2 + \frac{1}{2}\rho_{sB} (v_{sB} - v_n)^2 = \sqrt{\sigma F}, \quad (2)$$

where ρ_s , ρ_n , and v_s , v_n are the densities and velocities of

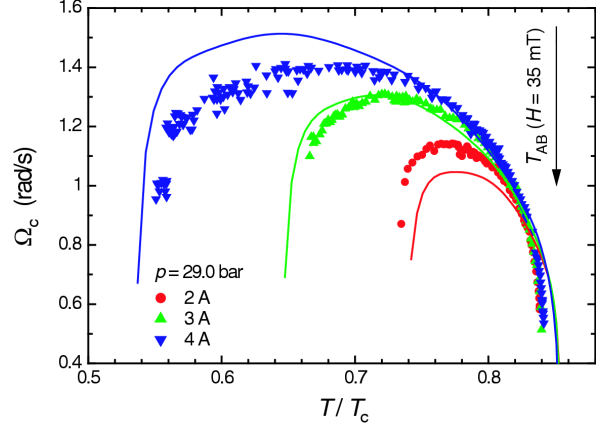


FIG. 4. Critical velocity Ω_c for the first appearance of B-phase vortex lines in the presence of the AB boundary as a function of temperature, while Ω is slowly increased ($\dot{\Omega} = 5 \cdot 10^{-4} \text{ rad/s}^2$). The current in the barrier solenoid is constant but different for the three sets of data. It controls the magnetic force F which is largely responsible for the shape of the curves. The solid curves represent Eq. (2) if one sets $\Omega_c = |v_{sB} - v_n|/R$ and $v_{sA} = v_n$. No fitting parameters are used. The values for $\sigma(T)$, $\chi_A - \chi_B(T, H)$, and $\rho_s(T)$ are obtained from accepted references [8,18–20], while H and ∇H apply for the profile $H(z)$ at the location of the AB boundary: $H_{AB}(T) = H(z)$.

superfluid and normal components [17]. In Fig. 4 we plot the prediction for the instability for three magnetic barrier profiles. With no fitting parameters the agreement with experiment is surprisingly good.

From Fig. 2 it is seen that of order $\delta N \approx 10$ vortex lines enter the B phase in one instability: in fact, at $0.77 T_c$ (with $u_c = 0.39 \text{ cm/s}$ at 29.0 bar) the measured average for more than 100 events is $\delta N \approx 11$. To compare with Eq. (2), δN corresponds to the number of circulation quanta $\kappa = h/2m_3$, which fit in one corrugation of the interface mode of size $\lambda_c/2 = \pi/k$. In practice, the counterflow $|v_{sA} - v_n|$ in A-phase is limited by the small critical velocity v_{cA} [13], and we may set $v_{sA} - v_n \approx 0$ in Eq. (2). In solid-body rotation there are then $N \approx \pi R^2 \Omega_c / \kappa$ vortex lines in the A phase which all flare out into the lateral sample boundary at the AB interface (Fig. 3A). Measured along the perimeter of the sample there are $\Omega_c R / \kappa$ circulation quanta per unit length and thus in one corrugation $\delta N \approx (\pi u_c) / (k \kappa)$. From Eq. (2) this is seen to be $\delta N \approx (2\pi\sigma) / (\kappa u_c \rho_{sB})$, which at $0.77 T_c$ gives 9 vortex lines in agreement with the measured number.

Eq. (2) has more interesting properties. As the normal components of both phases are in solid-body rotation and thus at rest in the rotating frame, it is the “superfluid winds” – the flow of the superfluid component, $|v_s - v_n|$, on each side of the interface – which produce the instability. It takes place even if the two superfluids have the same densities and velocities. In this sense it resem-

bles the flapping flag instability discussed by Rayleigh [3]: The role of the flagpole, which fixes the reference frame, falls here on the normal component, which moves with the rotating container.

It is interesting to compare Eqs. (1) and (2) in the low temperature limit, when $\rho_n \rightarrow 0$ and $\rho_{sA} \approx \rho_{sB} \rightarrow \rho$. We find that Eq. (2) gives a critical velocity which is by $\sqrt{2}$ smaller than that from Eq. (1). In fact, at $T = 0$ the valid condition is Eq. (1), since ρ_n is exactly zero and no normal component is left to provide a reference frame for the now undamped interface [17]. The ideal KH condition is then restored, as the only remaining drive is the velocity difference between the superfluid components. Not surprisingly, the two cases $\rho_n = 0$ and $\rho_n \rightarrow 0$ give different onsets for the instability: For a finite-size system the result would depend on the observation time – the time one waits for the interface to be coupled to the laboratory frame.

The shear-flow instability in superfluids thus provides an explicit bridge between the ideal inviscid and the viscous hydrodynamics. For two-fluid hydrodynamics it may have important consequences. It represents a new surface mechanism for vortex generation which might be applicable also to other interfaces, of which the normal state – superfluid boundary is of major interest. This interface occurs, for example, when the bulk superflow instability limit is reached in rotating $^3\text{He-B}$ at the sharpest surface spike on the lateral sample boundary [9]. A bubble of normal liquid is then created around this spike. Since the surrounding superflow moves at a high relative velocity, the bubble's interface may undergo a shear-flow instability and promote the generation of a vortex line.

A related case has been investigated in bulk $^3\text{He-B}$ which is in vortex-free rotation while it is irradiated with slow neutrons [21]. The absorption process of one neutron creates locally a bubble of $100\,\mu\text{m}$ size which is overheated up to the normal state. The bubble then quench cools back to the temperature of the surrounding superflow, as the normal–superfluid interface of the bubble contracts at high velocity. The measurements prove directly that vortices are formed in this rapid non-equilibrium transition and that the process is consistent with a volume effect known as the cosmological Kibble-Zurek (KZ) mechanism [22,23]. It has been suggested as the origin for cosmic-string formation when rapid non-equilibrium phase transitions swept across the Early Universe. The $^3\text{He-B}$ neutron experiment has been examined by solving analytically and numerically the time-dependent Ginzburg-Landau equation [24]. This study shows that in the non-equilibrium transition of the neutron bubble there exists also a competing surface mechanism, when the rapidly moving normal–superfluid interface becomes unstable and vortex rings form around the bubble in a corrugation instability. This is direct theoretical evidence for the existence of the shear-flow instability also at the normal–superfluid interface, between the

surrounding superflow and the stationary normal liquid within the bubble. A similar situation is the normal–superfluid boundary in a gaseous rotating Bose-Einstein condensate. Here the shear-flow instability also leads to a deformation of the surface of the condensate cloud by ripples and to vortex-line formation [25].

The shear-flow instability thus appears to be a universal surface mechanism for defect formation in superfluids and as intrinsic as the KZ mechanism in the bulk liquid. We are left to wonder whether or not these two are the only possible processes in the clean limit at the lowest temperatures, to which other observations of vortex formation can be reduced.

-
- [1] H. Lamb, *Hydrodynamics* (Dover Publ., New York, 1932), Chap. IX; S. Chandrasekhar, *Hydrodynamic and Hydromagnetic Stability* (Oxford University Press, New York, 1961), Chap. XI; L.D. Landau and E.M. Lifshitz, *Fluid Mechanics* (Pergamon Press, 1989), Chap. VII.
 - [2] Lord Kelvin (Sir William Thomson) *Mathematical and physical papers*, Vol. 4, *Hydrodynamics and General Dynamics*, Cambridge University Press, 1910.
 - [3] Lord Rayleigh (J.W. Strutt), *Scientific papers*, Vol. 1, Cambridge University Press, 1899.
 - [4] J. Zhang, S. Childress, A. Libchaber, M. Shelley, *Nature* **408**, 835 (2000).
 - [5] D.J. Goldfarb, B.J. Glasser, T. Shinbrot, *Nature* **415**, 302 (2002).
 - [6] H.L.F. von Helmholtz, *Monatsberichte der königlichen Akademie der Wissenschaften zu Berlin*, 215 (1868).
 - [7] G. Birkhoff, in *Hydrodynamic Instability*, Proc. Symp. Appl. Mathematics, Vol. XIII, edited by G. Birkhoff, R. Bellman, C. Lin, Amer. Math. Soc. 1962, p. 55.
 - [8] D. Vollhardt, P. Wölfe, *The Superfluid Phases of ^3He* (Taylor & Francis, London, 1990).
 - [9] Ü. Parts *et al.*, *Europhys. Lett.* **31**, 449 (1995); J. Low Temp. Phys. **107**, 93 (1997).
 - [10] R. Blaauwgeers *et al.*, *Nature* **404**, 471 (2000).
 - [11] P. Schiffer, D.D. Osheroff, *Rev. Mod. Phys.* **67**, 491 (1995).
 - [12] With only B phase in the sample, v_{cB} is determined by single-vortex formation at the sample boundary or by the leakage of vortices through the bottom orifice. Both processes differ in appearance from the events in Fig. 2.
 - [13] In this experiment the A-phase critical velocity is $v_{cA} \approx (0.36 \pm 0.06)\,\text{mm/s}$ [10].
 - [14] G.E. Volovik, *Physica B* **178**, 160 (1992).
 - [15] D.R. Tilley, J. Tilley, *Superfluidity and Superconductivity* (IOP Publ., Bristol, 1990).
 - [16] D.S. Buchanan, G.W. Swift, J.C. Wheatley, *Phys. Rev. Lett.* **57**, 341 (1986).
 - [17] More details on the calculation in: G.E. Volovik, preprint arXiv:cond-mat/0202445.
 - [18] D.D. Osheroff, M.C. Cross, *Phys. Rev. Lett.* **38**, 905 (1977).
 - [19] J.C. Wheatley, *Rev. Mod. Phys.* **47**, 415 (1975).
 - [20] Y.H. Tang, I. Hahn, H.M. Bozler, C.M. Gould, *Phys. Rev. Lett.* **67**, 1775 (1991).
 - [21] V.M.H. Ruutu, *et al.* *Nature* **382**, 334 (1996).

- [22] T.W.B. Kibble, J. Phys. A **9**, 1387 (1976).
- [23] W.H. Zurek, Nature **317**, 505 (1985).
- [24] I.S. Aranson, N.B. Kopnin, V.M. Vinokur, Phys. Rev. B **63**, 184501 (2001).
- [25] K.W. Madison, F. Chevy, V. Bretin, J. Dalibard, Phys. Rev. Lett. **86**, 4443 (2001).